

Engineered Ionic Gates for Ion Conduction Based on Sodium and Potassium Activated Nanochannels

Qian Liu,^{†,⊥} Kai Xiao,^{‡,⊥} Liping Wen,^{*,§} Heng Lu,[†] Yahui Liu,[†] Xiang-Yu Kong,[§] Ganhua Xie,[‡] Zhen Zhang,[‡] Zhishan Bo,^{*,†} and Lei Jiang^{§,‡}

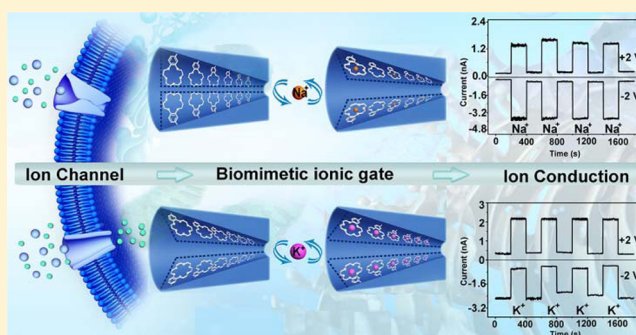
[†]Beijing Key Laboratory of Energy Conversion and Storage Materials, College of Chemistry, Key Laboratory of Theoretical and Computational Photochemistry, Ministry of Education, Beijing Normal University, Beijing 100875, PR China

[§]Laboratory of Bioinspired Smart Interfacial Science, Technical Institute of Physics and Chemistry, Chinese Academy of Sciences, Beijing 100190, PR China

[‡]Beijing National Laboratory for Molecular Sciences (BNLMS), Key Laboratory of Organic Solids, Institute of Chemistry, Chinese Academy of Sciences, Beijing 100190, PR China

Supporting Information

ABSTRACT: In living systems, ion conduction plays a major role in numerous cellular processes and can be controlled by biological ion channels in response to specific environmental stimuli. This article describes biomimetic ionic gates for ion conduction based on sodium and potassium activated nanochannels. The Na⁺ activated ionic gate and K⁺ activated ionic gate were developed by immobilizing the alkali metal cation-responsive functional molecules, 4'-aminobenzo-15-crown-5 and 4'-aminobenzo-18-crown-6, respectively, onto the conical polyimide nanochannels. When the ionic gate was in the presence of the specific alkali metal cation, positively charged complexes formed between the crown ether and the alkali metal cation. On the basis of the resulting changes in surface charge, wettability and effective pore size, the nanochannel can achieve reversible switching. The switching behaviors of the two complexes differed due to the differences in binding strength between the two complexes. The Na⁺ activated ionic gate is able to open and close to control the ion conduction through the nanochannel, and the K⁺ activated ionic gate enables selective cation and anion conduction through the nanochannel. The Na⁺ and K⁺ activated ionic gates show great promise for use in clinical medicine, biosensors and drug delivery based on their high sensitivity and selectivity of being activated, and good stability.



INTRODUCTION

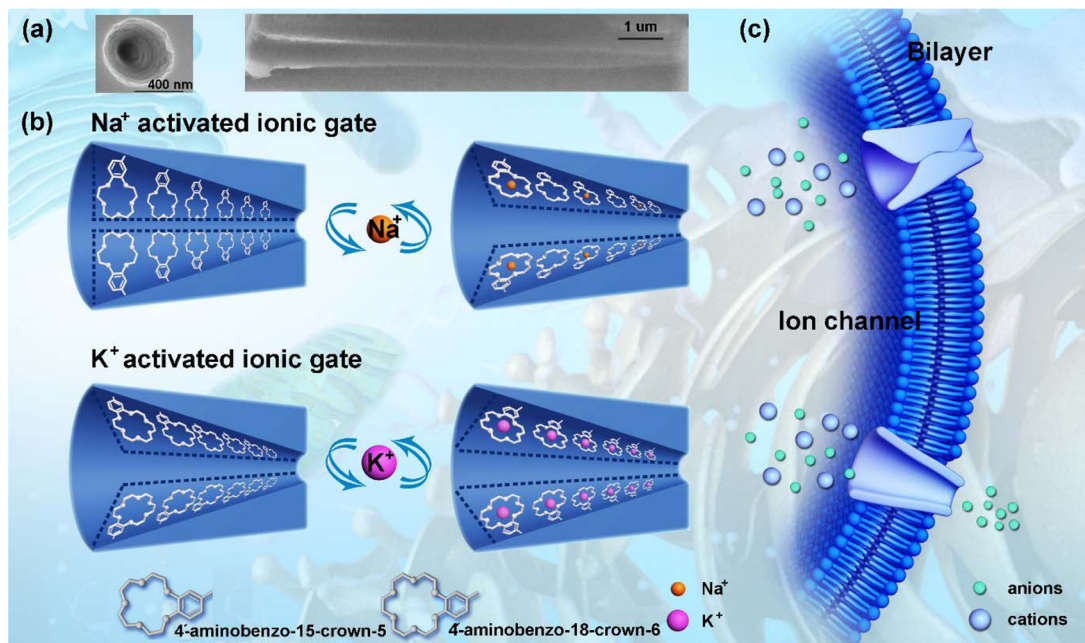
Biological ion channels are key components of cells and have many essential and remarkable properties.^{1,2} By continuously exchanging ions with the external environment, these ion channels perform a variety of essential functions in living organisms.^{3,4} For example, ion channels enable rapid ion conduction,⁵ and due to their high selectivity, they are able to discriminate between highly similar ion types and to display current rectification.^{6,7} Ion channel functions are regulated by the gating process, with environmentally responsive gates able to open and close the ion channel, controlling ion conduction in response to specific environmental stimuli.^{5,6} Ion conduction is important in numerous cellular processes, influencing electrolyte transport and the production of electrical signals in neurons.⁸ The remarkable features of biological ion channels provide an excellent source of inspiration for the development of biomimetic ion nanochannels.^{9–11} For example, Na⁺ and K⁺ are the most common and important ions in biological systems.^{12,13} Na⁺ regulates blood volume, blood pressure and osmotic equilibrium in humans. K⁺ is important in neuron

function, and impacts the osmotic equilibrium between cells and the interstitial fluid.^{14,15} It is generally considered quite difficult to distinguish between Na⁺ and K⁺ ions due to their similar physical and chemical properties. However, in living organisms, biological Na⁺ channels or K⁺ channels can efficiently discriminate Na⁺ or K⁺ from other alkali cations. Biological K⁺ channels can select K⁺ over Na⁺ with an efficiency of up to 1000:1, while Na⁺ channels efficiently discriminate Na⁺ from K⁺.^{16,17} Inspired by the biological K⁺ and Na⁺ channels, many researchers have attempted to produce selective ionic gates to regulate ion conduction based on biomimetic nanochannels responsive to Na⁺/K⁺.^{5,18–20}

In recent years, biomimetic nanochannels with simple structures and strong mechanical properties (such as supramolecular channels,^{21,22} carbon nanotubes,^{23,24} solid-state synthetic nanochannels^{25,26} and ion channels in artificial membrane materials²⁷ *etc.*) have developed rapidly in bionics.

Received: May 12, 2015

Published: September 4, 2015

Scheme 1. Na⁺ Activated Ionic Gate and K⁺ Activated Ionic Gate^a

^a(a) Enlarged SEM image of a single nanochannel viewed from its base, and the cross section of a typical conical PI nanochannel. (b) Schematic demonstration of the simplified Na⁺ activated ionic gate and K⁺ activated ionic gate. (c) Biomimetic Na⁺ and K⁺ activated nanochannels based on biological Na⁺ channels and K⁺ channels.

As various components of biological ion channels are asymmetric,²⁸ artificial biomimetic nanochannels with asymmetric structures have received more attention.^{29–32} Among these structures, solid-state synthetic nanochannels with conical structures have been extensively studied,³³ as they are relatively stable, flexible in terms of geometry and size, and amenable to surface functionalization.³⁴ Functionalized conical solid-state synthetic nanochannels can effectively respond to many environmental stimuli such as pH,³⁵ temperature,³⁶ ions,^{37,38} ligands,^{39,40} gas,⁴¹ light^{42,43} and even electric fields,⁴⁴ resulting in a wide range of potential applications in environmental monitoring, controlled nanofluids, filtration, nanomedicine and biosensors.^{45–47} Selective ionic gate to regulate ion conduction in response to Na⁺ or K⁺ in bionic systems can be obtained by combining Na⁺/K⁺-responsive molecules and conical solid-state synthetic nanochannels. Many Na⁺/K⁺-responsive molecules and functional groups have been reported, such as G-quadruplex DNA,⁴⁸ bioinspired graphene,⁵ calixarene,⁴⁹ hemispherands,^{50,51} amide⁵² and crown ethers.^{53,54} Crown ethers are attractive options due to their advantages of good solubility, simple chemical structure, good selectivity and ease of modification. Crown ethers have been widely researched as small organic molecules with special properties.^{55,56} Crown ethers have proven to be extremely useful ligands (hosts) for cations. The major reason for their selective cation binding is believed to be the relationship between the cation size and the crown ether cavity. Cations that match the crown ether cavity size are located in the center of the crown ethers, with optimal interactions with the oxygen heteroatoms.⁵⁷

Different from previous research,^{58,59} in this study, we combine crown ethers and a single conical polyimide (PI) nanochannel to obtain Na⁺/K⁺ activated ionic gates. These Na⁺ activated and K⁺ activated ionic gates not only have the advantages of their asymmetric solid-state synthetic nanochannel and crown ether components, but they can also

effectively regulate ion conduction in response to Na⁺ or K⁺ based on the association between Na⁺/K⁺ and crown ethers in bionic systems. On the basis of the selectivity of crown ethers to alkali metal cations,^{60,61} we produce a Na⁺ activated ionic gate and a K⁺ activated ionic gate, obtained by separately immobilizing 4'-aminobenzo-15-crown-5 (4-AB15C5) and 4'-aminobenzo-18-crown-6 (4-AB18C6) onto a single conical PI nanochannel. For a conical PI nanochannel (as shown in Scheme 1a), ionic current rectification emerges due to the intrinsic shape and asymmetric electrochemical potential, which can preferentially transport anions/cations from the small opening (tip) to the large opening (base) of the nanochannel.^{62,63} The current values can be visualized by measuring the current–voltage (*I*–*V*) curves under the condition of symmetrical electrolyte concentrations. The current values are mainly influenced by the charge of the inner surface, which reflects the ion conduction.⁶⁴ With a positively charged inner surface, the current values at positive voltage are greater than those at negative voltage, indicating the nanochannel mainly supports anion conduction; alternatively, current values at a positive voltage that are less than those at a negative voltage under the condition of a negatively charged inner surface indicates that the nanochannel mainly supports cation conduction (Figure S1 in Supporting Information).

As shown in Scheme 1b, the Na⁺ activated and K⁺ activated ionic gates were obtained by preparing 4-AB15C5-modified and 4-AB18C6-modified nanochannels, respectively. As Na⁺ has an ionic radius of 0.98 Å, it forms a very stable complex with 15-crown-5, which has a cavity with a similar radius (0.86–1.1 Å).⁵⁷ For the Na⁺ activated ionic gate, after modification with 4-AB15C5, the nanochannel presents the “off” state. Thereafter, activation with Na⁺ induces the “on” state of the nanochannel. Alternately introducing and removing Na⁺ demonstrates the reversibility of the on/off property. Meanwhile 18-crown-6 selects K⁺ over Na⁺ in aqueous solutions because of its size

compatibility (the radius of K^+ is 1.38 Å, while the radius of the 18-crown-6 cavity is 1.3–1.6 Å), and greater free energy of binding.^{56,65} For the K^+ activated ionic gate, the nanochannel is in the “on” state after modification with 4-AB18C6, and the ionic gate takes on the reverse “on” state when activated by K^+ . Moreover, these Na^+ activated and K^+ activated ionic gates could be employed in bionic systems as shown in Scheme 1c. These biological ion channels could be applied in living organisms to control ion conduction after activation with Na^+ and K^+ .

RESULTS AND DISCUSSION

Current measurements were used to examine the current–voltage (I – V) characteristics of single PI nanochannels after modification with 4-AB15C5/4-AB18C6 (Figure S2 in Supporting Information) before and after activation with Na^+/K^+ . As shown in Figure 1a, the current of 4-AB15C5-

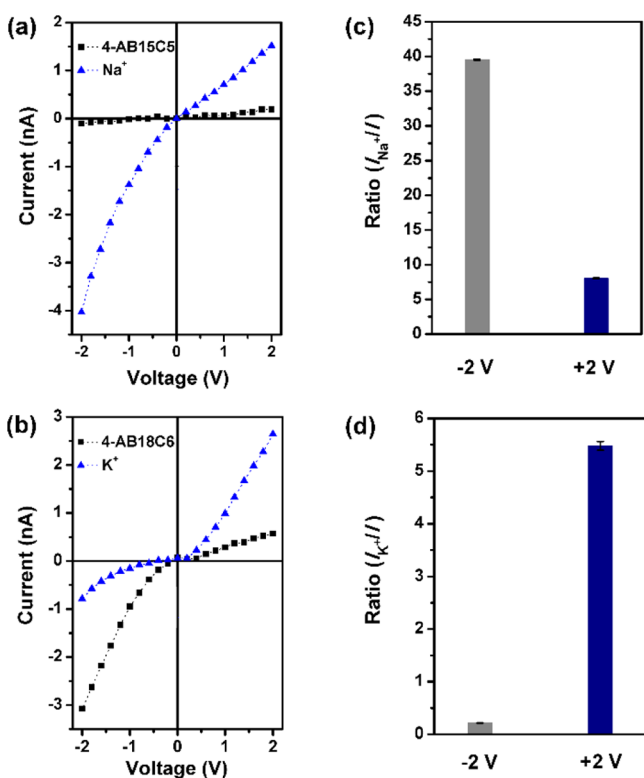


Figure 1. Asymmetric ionic transport properties of the Na^+ activated and K^+ activated ionic gates in 0.1 M Tris-HCl (pH 4.5): (a) current–voltage characteristics of the 4-AB15C5-modified nanochannel before (black square) and after (navy triangle) activation with $10 \mu\text{M } Na^+$; (b) current–voltage characteristics of the 4-AB18C6-modified nanochannel before (black square) and after (navy triangle) activation with $10 \mu\text{M } K^+$; (c) the current ratios (I_{Na^+}/I) of 4-AB15C5-modified nanochannels after activation with $10 \mu\text{M } Na^+$ at -2.0 V (gray column) and $+2.0$ V (navy column); (d) the current ratios (I_{K^+}/I) of 4-AB18C6-modified nanochannel after activation with $10 \mu\text{M } K^+$ at -2.0 V (gray column) and $+2.0$ V (navy column), respectively.

modified single PI nanochannel is very low, indicating the nanochannel is in the “off” state without ion conduction. When Na^+ is added to activate the 4-AB15C5-modified nanochannel, the current increases dramatically from about -0.1 to -4.2 nA at -2.0 V and about $+0.2$ to $+1.6$ nA at $+2.0$ V. The nanochannel is in the “on” state at both ends of the 4-AB15C5-modified nanochannel, enabling the conduction of anions and

cations through the nanochannel. This behavior could be explained by the variations in effective pore size, wettability, and surface charge in response to Na^+ binding.^{66,67} After modification with 4-AB15C5, the ionic current through the nanochannel is low due to the generation of less charged surface in the tip of nanochannel together with the decrease of the effective pore size. It results in the “off” state. When Na^+ binds to 4-AB15C5 immobilized in the nanochannel, the hydrophobicity of the nanochannel increases slightly as demonstrated by the contact angle measurements on flat PI films (Figure S3 in Supporting Information), which would cause a decrease in current. However, surface charge exerts the dominant effect on the change of current. The surface charge of the nanochannel changes to be more positive with the formation of positively charged complex between 4-AB15C5 and Na^+ . Meanwhile, the incomplete modification of the nanochannel by crown ether leads to the residual negative charge. The cooperation effect of surface charge and wettability results in a clear increase in the current through the nanochannel, switching the Na^+ activated ionic gate to the “on” state.

The 4-AB18C6-modified single PI nanochannel exhibits a different phenomenon upon K^+ activation. As shown in Figure 1b, after 4-AB18C6 modification, the single PI nanochannel exhibits a rectified I – V curve, mainly allowing cation conduction. This is because although the surface charge changes to neutral, 4-AB18C6 is more hydrophilic than 4-AB15C5 as demonstrated by the contact angle measurements on PI film after modification with 4-AB15C5 and 4-AB18C6 (Figure S3 in the Supporting Information). Meanwhile, compared to 4-AB15C5, less 4-AB18C6 is immobilized on the surface of the nanochannel due to its larger size, leading to more residual negative charge in the nanochannel. As a result, the 4-AB18C6-modified nanochannel exhibits an “on” state with a rectified I – V curve. When K^+ is added to the 4-AB18C6-modified nanochannel, a distinct reversal occurs, with the current decreasing from about -3.4 to -0.9 nA at -2.0 V and increasing from about $+0.5$ to $+2.7$ nA at $+2.0$ V. This sharp increase in the positive surface charge causes the reversal of current, mainly resulting in anion conduction. Figure 1c and Figure 1d express the current ratios (I_{Na^+}/I and I_{K^+}/I) of the 4-AB15C5-modified nanochannel and the 4-AB18C6-modified nanochannel, which are calculated as the current after activation with alkali metal cations (Na^+ and K^+) divided by the current before activation with alkali metal cations at -2.0 V (or $+2.0$ V). A dramatic difference in the current ratios was observed between the Na^+ activated ionic gate (~ 40 at -2.0 V and ~ 8 at $+2.0$ V) and the K^+ activated ionic gate (~ 0.2 at -2.0 V and ~ 5.4 at $+2.0$ V). Therefore, these results indicate that Na^+ can efficiently control the “off” and “on” states of ion conduction in 4-AB15C5-modified nanochannels, and K^+ can control the selective cation or anion conduction in 4-AB18C6-modified nanochannels.

The concentrations of alkali metal cations (Na^+ and K^+) affect the extent of the Na^+ activated and K^+ activated ionic gates in the “on” state as expressed by the current through the crown ether (4-AB15C5 and 4-AB18C6)-modified nanochannels. Figure 2a shows the current variation of the 4-AB15C5-modified nanochannel under constant voltage ($+2.0$ V and -2.0 V) after activation with Na^+ concentrations from 1 nM to 100 mM. Before activation with Na^+ , the current through the 4-AB15C5-modified nanochannel is about $+0.5$ nA at a constant voltage of $+2.0$ V and -0.2 nA at a constant

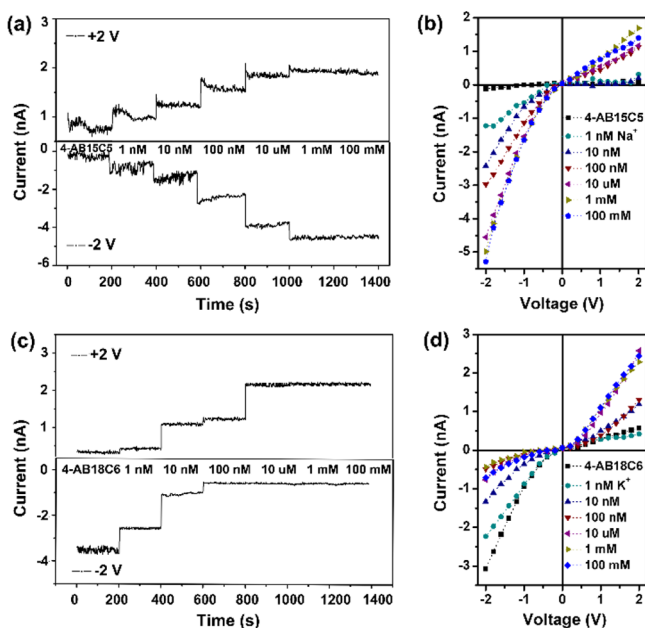


Figure 2. Dependence of the Na^+ activated (a and b) and K^+ activated ionic gates (c and d) on the alkali metal cation concentrations (from 1 nM to 100 mM): (a) the current variation of the 4-AB15C5-modified nanochannels before and after activation with different concentrations of Na^+ at constant voltage +2.0 V (up) and -2.0 V (down); (b) I - V characteristics of the 4-AB15C5-modified nanochannel before and after activation with different Na^+ concentrations; (c) the current variation of the 4-AB18C6-modified nanochannel before and after activation with different concentrations of K^+ at a constant voltage of +2.0 V (up) and -2.0 V (down); (d) I - V characteristics of the 4-AB18C6-modified nanochannel before and after activation with different K^+ concentrations.

voltage of -2.0 V. When the 4-AB15C5-modified nanochannel was activated with different concentrations of Na^+ (from 1 nM to 1 mM), the current at a constant voltage of +2.0 V increased gradually from about +1.0 to +2.0 nA, and the current at a constant voltage of -2.0 V increased from about -1.2 to -4.5 nA. At higher Na^+ concentrations (from 1 mM to 100 mM), the current at +2.0 and -2.0 V leveled off around +2.0 and -4.5 nA. This phenomenon is also reflected by the I - V characteristics of the 4-AB15C5-modified nanochannel after activation with various concentrations of Na^+ , as shown in Figure 2b.

For the K^+ activated ionic gate, the K^+ concentration also exerts a clear influence on the current value at constant voltage (+2.0 and -2.0 V). As shown in Figure 2c, at a constant voltage of +2.0 V, the current through the 4-AB18C6-modified nanochannel increases from about +0.3 to +2.1 nA as the K^+ concentration increases from 1 nM to 10 μM , and the current remains constant at higher K^+ concentrations (1 μM to 100 mM). However, the variation in the current at a constant voltage of -2.0 V followed a different trend. When different concentrations of K^+ were added from 1 nM to 100 nM, the current first decreased from about -3.5 to -0.5 nA and then remained unchanged at higher K^+ concentrations (from 100 nM to 100 mM). This current reversal can be better visualized by the I - V characteristics of the 4-AB18C6-modified nanochannel after activation with different K^+ concentrations (as shown in Figure 2d).

The influence of alkali metal cation (Na^+ and K^+) concentrations on the Na^+ activated and K^+ activated ionic

gates can be attributed to changes in the surface charge and wettability. At low concentrations of alkali metal cations (Na^+ or K^+), the current through the crown ether (4-AB15C5 or 4-AB18C6)-modified nanochannels changes, mainly due to the increasing positive charge caused by the binding of the alkali metal cations (Na^+ or K^+) to the crown ethers (4-AB15C5 or 4-AB18C6). When all of the crown ether (4-AB15C5 or 4-AB18C6) has combined with alkali metal cations (Na^+ or K^+), the current reaches its maximum value and remains unchanged by the addition of more alkali metal cations (Na^+ or K^+) due to the saturation of the positive surface charge and the wettability equilibration.

The selective activation of 4-AB15C5-modified and 4-AB18C6-modified nanochannels with alkali metal cations (Li^+ , Na^+ and K^+) are shown in Figure 3. The selective

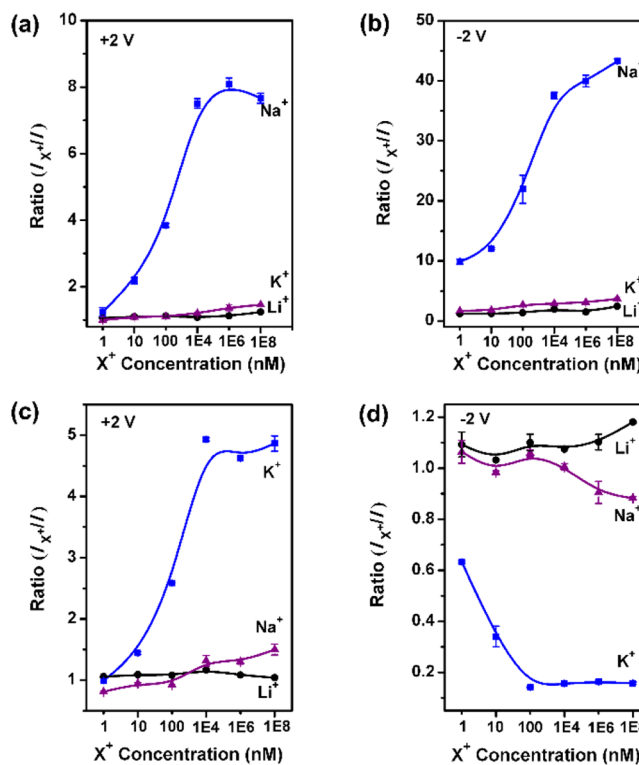


Figure 3. Selective activation of 4-AB15C5-modified and 4-AB18C6-modified nanochannels with alkali metal cations: the current ratios (I_{X^+}/I) of the 4-AB15C5-modified nanochannel after activation with different concentrations (from 1 nM to 100 mM) of Li^+ (black circle), Na^+ (navy square) and K^+ (purple triangle) at +2.0 V (a) and -2.0 V (b); the current ratios I_{X^+}/I of the 4-AB18C6-modified nanochannel after activation with different concentrations (from 1 nM to 100 mM) of Li^+ (black circle), Na^+ (purple triangle) and K^+ (navy square) at +2.0 V (c) and -2.0 V (d).

activation can be expressed by the current ratio I_{X^+}/I , which is calculated as the current of the crown ether (4-AB15C5 or 4-AB18C6)-modified nanochannel after activation with alkali metal cations (Li^+ , Na^+ and K^+) divided by the current before activation with alkali metal cations at +2.0 or -2.0 V. For the Na^+ activated ionic gate (as shown in Figure 3a and Figure 3b), the current ratios changed significantly, increasing from about 1.3 to 8.1 at +2.0 V and increasing from about 9.8 to 43.3 at -2.0 V as the concentration of Na^+ increased from 1 nM to 100 mM. In contrast, the current ratios changed only slightly upon the addition of Li^+ and K^+ . As the sizes of Li^+ and K^+ do not

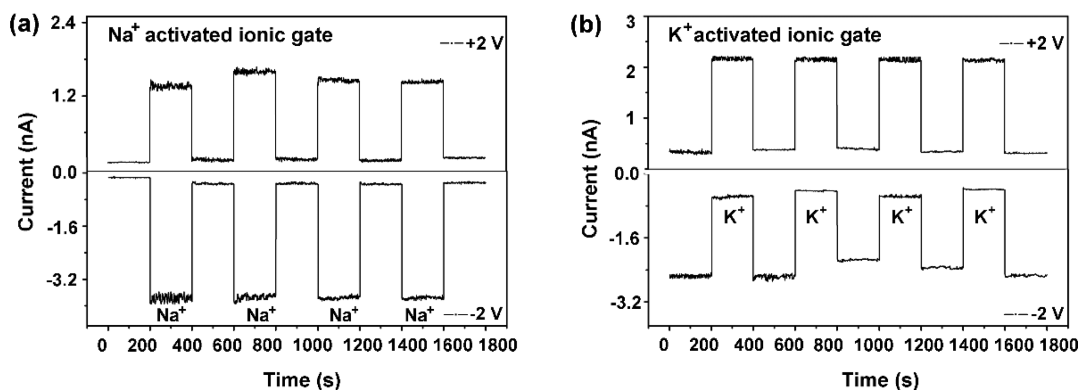


Figure 4. Stability and responsive switchability of the Na⁺ activated and K⁺ activated ionic gates: (a) the variation in the reversible ionic currents of the 4-AB15C5-modified nanochannel measured alternately at a constant voltage of +2.0 V (up) and -2.0 V (down) in the presence of Na⁺ and [2.2.2]-cryptand; (b) the variation in the reversible ionic currents of the 4-AB18C6-modified nanochannel measured alternately at a constant voltage of +2.0 V (up) and -2.0 V (down) in the presence of K⁺ and [2.2.2]-cryptand.

match the 4-AB15C5 cavity size, these ions cannot induce significant changes in the surface charge or wettability of the 4-AB15C5-modified nanochannel. These results indicate that as a Na⁺ activated ionic gate, the 4-AB15C5-modified nanochannel can only be selectively activated by Na⁺.

As a K⁺ activated ionic gate, the 4-AB18C6-modified nanochannel also can only be selectively activated by K⁺ due to the match between the size of K⁺ and the size of the 4-AB18C6 cavity. Figure 3c and 3d show the selectivity of the 4-AB18C6-modified nanochannel to Li⁺, Na⁺ and K⁺. The change in the current ratio after interaction with K⁺ was greater than that observed for Li⁺ and Na⁺. At +2.0 V, the current ratio increased from about 1 to 5 and leveled off at approximately 5, and at -2.0 V it decreased from about 0.7 to 0.2 and leveled off at approximately 0.2 as the concentration of K⁺ increased from 1 nM to 100 mM. However, the current ratios at both +2.0 V and -2.0 V only increased to a small degree in response to the addition of Na⁺ or Li⁺. This result indicates that K⁺ has a high selectivity for the activation of the 4-AB18C6-modified nanochannel. In a solution of Na⁺ and K⁺, the Na⁺ (or K⁺) activated ionic gate also shows good selectivity of being activated and stability (Figure S10 and Figure S11 in the Supporting Information).

Both the Na⁺ activated and K⁺ activated ionic gates also exhibit good stability and responsive switchability. The cycling performance of the Na⁺ activated and K⁺ activated ionic gates can be reflected by the change in the current through the crown ether (4-AB15C5 or 4-AB18C6)-modified nanochannels under constant voltage (+2.0 V and -2.0 V). The reversibility of the two ionic gates can be realized by the addition of [2.2.2]-cryptand to the crown ether (4-AB15C5 or 4-AB18C6)-modified nanochannel. In water, [2.2.2]-cryptand has a much higher binding constant with Na⁺ than 15-crown-5 and with K⁺ than 18-crown-6.⁶⁸ As shown in Figure 4a, the current of the 4-AB15C5 modified nanochannel was about +1.3 nA at +2.0 V and -3.8 nA at -2.0 V in the presence of Na⁺. After the nanochannel was soaked in 0.1 M [2.2.2]-cryptand aqueous solution, the current decreased to about +0.2 nA and -0.2 nA, respectively. Under these conditions, the "on" state and "off" state can be activated simultaneously at both ends of the 4-AB15C5-modified nanochannel. Several cycles later, no damping of the ionic current is observed, indicating that the Na⁺ activated ionic gate has good stability and cycling performance to regulate the ion conduction of the nanochannel. Similar to

the Na⁺ activated ionic gate, the K⁺ activated ionic gate also exhibits stability and cyclical selectivity for anion and cation conduction. As shown in Figure 4b, the current of the 4-AB18C6-modified nanochannel was about +2.1 nA at +2.0 V and -0.4 nA at -2.0 V in the presence of K⁺, with mainly anion conduction occurring through the nanochannel. However, in the presence of [2.2.2]-cryptand, the current decreased to about +0.4 nA at +2.0 V and increased to -2.6 nA at -2.0 V, with mainly cation conduction occurring through the nanochannel. No damping of the ionic current is observed after several cycles.

Moreover, to explain the difference between the Na⁺ activated and K⁺ activated ionic gates, the association constants of 4-AB15C5 ⊃ Na⁺ (as shown in Figure 5a) and 4-AB18C6 ⊃ K⁺ (as shown in Figure 5b) were measured by ¹H NMR titration. We chose 4-AB15C5 or 4-AB18C6 as model hosts, and Na⁺ and K⁺ as model guests to compare the binding strengths between 4-AB15C5 ⊃ Na⁺ and 4-AB18C6 ⊃ K⁺. The concentration-dependent ¹H NMR spectra of 4-AB15C5 ⊃ Na⁺ (Figure 5c) and 4-AB18C6 ⊃ K⁺ (Figure 5d) indicate their associative behaviors.^{69,70} As the concentration of guests (Na⁺ and K⁺) increased, the signals of protons H₄ on 4-AB15C5 and protons H₅ on 4-AB18C6 shifted downfield, indicating the introduction of the electron withdrawing group (Na⁺ and K⁺). The mole ratio plots based on proton NMR data showed that the complexes of 4-AB15C5 and Na⁺, 4-AB18C6 and K⁺ were both 1:1 stoichiometry in water at room temperature (as shown in Figure 5e). A nonlinear curve-fitting method (Equation S2 in Supporting Information)^{71,72} was used to determine the association constant of 4-AB15C5 ⊃ Na⁺ by ¹H NMR titration as 13.2 M⁻¹, which is about half the association constant of 4-AB18C6 ⊃ K⁺ (23.3 M⁻¹) in water (Figure 5f). Therefore, K⁺ activated ionic gate have a far greater positive surface charge than the Na⁺ activated ionic gate after activation with their respective alkali metal cations (Na⁺ or K⁺). Meanwhile, the incomplete modification with crown ether results in residual negative charge in the nanochannel. Because of the complicated situation in the surface including charge and wettability, the K⁺ activated ionic gate exhibits current reversal after activation with K⁺, while the Na⁺ activated ionic gate does not after activation with Na⁺ (Figure S12 in the Supporting Information).

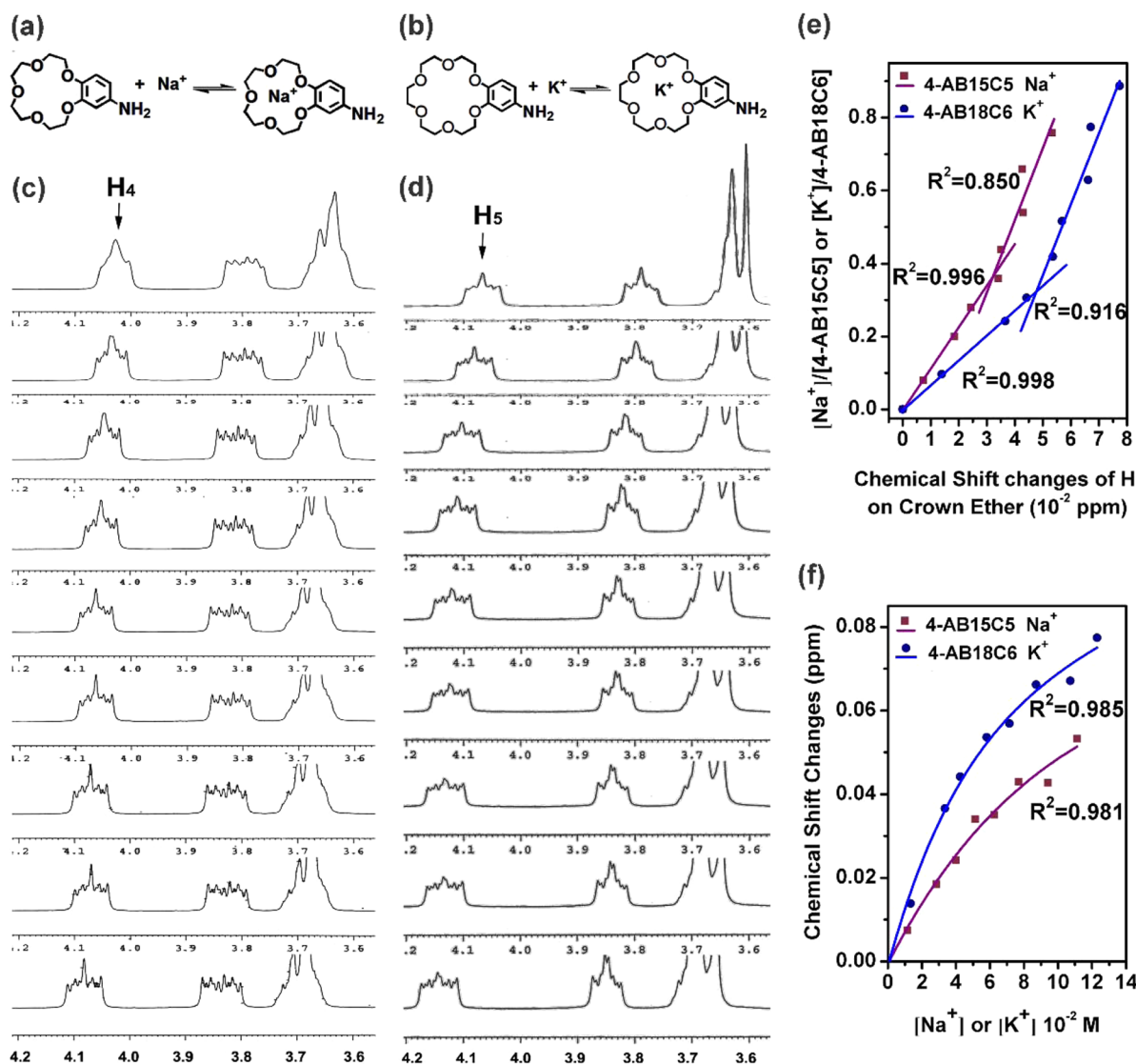


Figure 5. Association constant determination for the complex formation between 4-AB15C5 and Na⁺, and between 4-AB18C6 and K⁺ in water solution: (a) chemical reaction equation of 4-AB15C5 and Na⁺; (b) chemical reaction equation of 4-AB18C6 and K⁺; (c) partial ¹H NMR spectra (300 MHz, D₂O, room temperature) of 4-AB15C5 (30 mM) upon the addition of Na⁺ (from top to bottom: 0.00, 11.4, 28.5, 40.0, 51.3, 62.7, 77.0, 94.1, 111.2 mM); (d) partial ¹H NMR spectra (300 MHz, D₂O, room temperature) of 4-AB18C6 (32.00 mM) upon the addition of K⁺ (from top to bottom: 0.00, 13.4, 33.5, 42.5, 58.1, 71.5, 87.2, 107.3, 123.0 mM); (e) mole ratio plot for 4-AB15C5 and Na⁺ (purple square and purple line), and 4-AB18C6 and K⁺ (navy circle and navy line), indicating the 1:1 stoichiometry; (f) chemical shift changes of H₄ on 4-AB15C5 upon the addition of Na⁺ (purple square and purple line), and chemical shift changes of H₅ on 4-AB18C6 upon the addition of K⁺ (navy circle and navy line).

CONCLUSIONS

In summary, novel Na⁺ activated and K⁺ activated ionic gates that control anion and cation conduction through nano-channels were successfully realized by immobilizing 4'-amino-benzo-15-crown-5 and 4'-amino-benzo-18-crown-6 onto single ion track-etched conical nanochannels. The presence of Na⁺ switches the Na⁺ activated ionic gate between the "off" and "on" states of ion conduction, and the presence of K⁺ controls selective cation and anion conduction through the K⁺ activated ionic gate. These two alkali metal cation (Na⁺ and K⁺) activated ionic gates not only have high sensitivity and selectivity of being activated, but they also exhibit excellent responsive switchability and stability. Moreover, These Na⁺ activated and K⁺ activated ionic gates hold great promise for application in living and bionic systems (such as clinical medicine, biosensors and drug delivery).

EXPERIMENTAL SECTION

Materials. Polyimide (PI, Hostaphan RN12 Hoechst, 12- μ m thick) film, 4'-aminobenzo-15-crown-5 and 4'-aminobenzo-18-crown-6, N-hydroxysulfosuccinimide (NHSS), 1-Ethyl-3-(3-dimethylaminopropyl) carbodiimide (EDC), Tris-HCl, potassium chloride (KCl), sodium chloride (NaCl), lithium chloride (LiCl), potassium iodide (KI) and sodium hypochlorite (NaClO, 13%) were purchased from Sinopharm Chemical Reagent Beijing Co., Ltd. (SCRC, China) and J&K Beijing Co., Ltd. All solutions were prepared in Milli-Q water (18.2 M Ω).

Fabrication. The single conical PI nanochannels were prepared by an asymmetric track-etched technique with a single ion track. Prior to the etching process, each side of the PI films was exposed to UV light (320 nm) for 1 h. The PI films were embedded between the two chambers of a conductivity cell at 60 °C. One chamber was filled with etching solution (NaClO, 13%), while the other chamber was filled with stopping solution (1 M KI). Then, a constant voltage of 1.0 V was applied across the films. The etching process was stopped at a desired current value corresponding to a certain tip diameter. Then the

etching solution was removed and two chambers were filled with stopping solution for 1 h. After that, the nanochannel was immersed in distilled water waiting for being modified. This work used 12 single conical PI nanochannels. The base diameter of the single conical PI nanochannels was approximately 600 nm, and the tip diameter was calculated to be ~ 10 nm.

Modification. After chemical etching, the carboxyl groups were exposed on the nanochannel surface, and then 4-AB15C5 or 4-AB18C6 was immobilized on the nanochannel surface by a conventional EDC/NHSS coupling reaction. The NHSS ester was formed by soaking the PI films in a 2 mL aqueous solution of 30 mg EDC and 6 mg NHSS for 1 h. Then, the PI films were washed and treated with 10 mM 4-AB15C5 or 4-AB18C6 aqueous solution overnight. Finally, the 4-AB15C5 or 4-AB18C6-modified films were washed three times with distilled water.

Activation. After modification, the crown ether (4-AB15C5 or 4-AB18C6)-modified nanochannel was activated by immersing in a solution of 10 μ M Na⁺ (or K⁺). Then, the Na⁺ (or K⁺) activated nanochannel was washed three times with distilled water.

Current Measurement. Current–voltage characteristics were measured with a Keithley 6487 picoammeter (Keithley Instruments, Cleveland, OH). The asymmetric ionic transport properties of the Na⁺ activated and K⁺ activated ionic gates were evaluated by the current–voltage (I – V) curves that were constructed using 0.1 M Tris-HCl (pH 4.5) as the electrolyte. A single conical PI nanochannel was mounted between two chambers of the etching cell mentioned above. Ag/AgCl electrodes were used to apply a transmembrane potential through the nanochannel. Experiments were performed with transmembrane potentials of a scanning voltage varying from -2.0 to $+2.0$ V with a 21 s period, and a constant voltage of $+2.0$ or -2.0 V. All measurements were carried out at room temperature.

NMR Spectra. ¹H NMR spectra (D₂O, 298 K) were recorded on a Bruker DM300 or AV 400 spectrometer with TMS as the internal standard. All chemical shifts were quoted in parts per million (ppm).

SEM Measurement. Scanning electron microscopy (SEM) measurements were captured in the field-emission mode using a Hitachi S-4800 microscope at an acceleration voltage of 5 kV.

Contact Angle Measurement. Contact angles were measured by an OCA20 instrument (DataPhysics, Germany).

XPS Measurement. X-ray photoelectron spectra (XPS) data were obtained by an ESCALab220i-XL electron spectrometer from VG Scientific set to 300 W Al K α radiation.

■ ASSOCIATED CONTENT

● Supporting Information

The Supporting Information is available free of charge on the ACS Publications website at DOI: 10.1021/jacs.5b04911.

Contact angles, X-ray photoelectron spectra (XPS) data, current–voltage (I – V) curves demonstrating the selective activation and cycling performance of the Na⁺ and K⁺ activated ionic gates, diameter dependence of the Na⁺ activated ionic gate, the channel-to-channel variability, the detailed process of calculating the association constant, corresponding schematic representations of the surface states in nanochannels after modification and activation, rectification mechanism, and competitive binding in a solution of Na⁺ and K⁺. (PDF)

■ AUTHOR INFORMATION

Corresponding Authors

*wen@mail.ipc.ac.cn

*zsbo@bnu.edu.cn

Author Contributions

[†]These authors contributed equally.

Notes

The authors declare no competing financial interest.

■ ACKNOWLEDGMENTS

This work was supported by the National Research Fund for Fundamental Key Projects (2011CB935702), the National Natural Science Foundation (21171171, 21434003, 91427303, 91127025), and the Key Research Program of the Chinese Academy of Sciences (KJZD-EW-M01, KJZD-EW-M03).

■ REFERENCES

- (1) Fyles, T. M. *Chem. Soc. Rev.* **2007**, *36*, 335.
- (2) de la Escosura-Muñiz, A.; Merkoçi, A. *ACS Nano* **2012**, *6*, 7556.
- (3) Wickenden, A. D. *Pharmacol. Ther.* **2002**, *94*, 157.
- (4) Xia, H.; Qin, D. D.; Zhou, X. B.; Liu, X. H.; Lu, X. Q. *J. Phys. Chem. C* **2013**, *117*, 23522.
- (5) He, Z. J.; Zhou, J.; Lu, X. H.; Corry, B. *ACS Nano* **2013**, *7*, 10148.
- (6) Agre, P. *Angew. Chem., Int. Ed.* **2004**, *43*, 4278.
- (7) MacKinnon, R. *Angew. Chem., Int. Ed.* **2004**, *43*, 4265.
- (8) Schmalhofer, W. A.; Sanchez, M.; Dai, G.; Dewan, A.; Secades, L.; Hanner, M.; Knaus, H.-G.; McManus, O. B.; Kohler, M.; Kaczorowski, G. J.; Garcia, M. L. *Biochemistry* **2005**, *44*, 10135.
- (9) Plesa, C.; Dekker, C. *Nanotechnology* **2015**, *26*, 084003.
- (10) Howorka, S.; Siwy, Z. S. *Chem. Soc. Rev.* **2009**, *38*, 2360.
- (11) Siwy, Z. S.; Howorka, S. *Chem. Soc. Rev.* **2010**, *39*, 1115.
- (12) Lifton, R. P.; Gharavi, A. G.; Geller, D. S. *Cell* **2001**, *104*, 545.
- (13) Chambrey, R.; Trepiccione, F. *Curr. Hypertens. Rep.* **2015**, *17*, 1.
- (14) Brickley, S. G.; Revilla, V.; Cull-Candy, S. G.; Wisden, W.; Farrant, M. *Nature* **2001**, *409*, 88.
- (15) Danbolt, N. C. *Prog. Neurobiol.* **2001**, *65*, 1.
- (16) Favre, I.; Moczydlowski, E.; Schild, L. *Biophys. J.* **1996**, *71*, 3110.
- (17) Payandeh, J.; Scheuer, T.; Zheng, N.; Catterall, W. A. *Nature* **2011**, *475*, 353.
- (18) Assouma, C. D.; Crochet, A.; Chérémond, Y.; Giese, B.; Fromm, K. M. *Angew. Chem., Int. Ed.* **2013**, *52*, 4682.
- (19) Gong, X. J.; Li, J. C.; Xu, K.; Wang, J. F.; Yang, H. *J. Am. Chem. Soc.* **2010**, *132*, 1873.
- (20) Hou, X.; Guo, W.; Xia, F.; Nie, F. Q.; Dong, H.; Tian, Y.; Wen, L. P.; Wang, L.; Cao, L. X.; Yang, Y.; Xue, J. M.; Song, Y. L.; Wang, Y. G.; Liu, D. S.; Jiang, L. *J. Am. Chem. Soc.* **2009**, *131*, 7800.
- (21) Matile, S.; Vargas Jentzsch, A.; Montenegro, J.; Fin, A. *Chem. Soc. Rev.* **2011**, *40*, 2453.
- (22) Chui, J. K. W.; Fyles, T. M. *Chem. Soc. Rev.* **2012**, *41*, 148.
- (23) Shao, Q.; Zhou, J.; Lu, L. H.; Lu, X. H.; Zhu, Y. D.; Jiang, S. Y. *Nano Lett.* **2009**, *9*, 989.
- (24) Wan, R. Z.; Li, J. Y.; Lu, H. J.; Fang, H. P. *J. Am. Chem. Soc.* **2005**, *127*, 7166.
- (25) Dekker, C. *Nat. Nanotechnol.* **2007**, *2*, 209.
- (26) Plesa, C.; van Loo, N.; Ketterer, P.; Dietz, H.; Dekker, C. *Nano Lett.* **2015**, *15*, 732.
- (27) Kawano, R.; Osaki, T.; Sasaki, H.; Takinoue, M.; Yoshizawa, S.; Takeuchi, S. *J. Am. Chem. Soc.* **2011**, *133*, 8474.
- (28) Gouaux, E.; MacKinnon, R. *Science* **2005**, *310*, 1461.
- (29) Ali, M.; Yameen, B.; Neumann, R.; Ensinger, W.; Knoll, W.; Azzaroni, O. *J. Am. Chem. Soc.* **2008**, *130*, 16351.
- (30) Pérez-Mitta, G.; Tuninetti, J. S.; Knoll, W.; Trautmann, C.; Toimil-Molares, M. E.; Azzaroni, O. *J. Am. Chem. Soc.* **2015**, *137*, 6011.
- (31) Martin, C. R.; Siwy, Z. S. *Science* **2007**, *317*, 331.
- (32) Wang, G. L.; Zhang, B.; Wayment, J. R.; Harris, J. M.; White, H. S. *J. Am. Chem. Soc.* **2006**, *128*, 7679.
- (33) Hou, X.; Guo, W.; Jiang, L. *Chem. Soc. Rev.* **2011**, *40*, 2385.
- (34) Zhang, H. C.; Hou, X.; Yang, Z.; Yan, D. D.; Li, L.; Tian, Y.; Wang, H. T.; Jiang, L. *Small* **2015**, *11*, 786.
- (35) Xiao, K.; Xie, G.; Li, P.; Liu, Q.; Hou, G. L.; Zhang, Z.; Ma, J.; Tian, Y.; Wen, L. P.; Jiang, L. *Adv. Mater.* **2014**, *26*, 6560.
- (36) Yameen, B.; Ali, M.; Neumann, R.; Ensinger, W.; Knoll, W.; Azzaroni, O. *Small* **2009**, *5*, 1287.
- (37) Liu, Q.; Xiao, K.; Wen, L. P.; Dong, Y.; Xie, G. H.; Zhang, Z.; Bo, Z. S.; Jiang, L. *ACS Nano* **2014**, *8*, 12292.
- (38) Siwy, Z. S.; Powell, M. R.; Petrov, A.; Kalman, E.; Trautmann, C.; Eisenberg, R. S. *Nano Lett.* **2006**, *6*, 1729.

- (39) Sun, Z. Y.; Zhang, F.; Zhang, X. Y.; Tian, D. M.; Jiang, L.; Li, H. *B. Chem. Commun.* **2015**, *51*, 4823.
- (40) Xie, G. H.; Tian, W.; Wen, L. P.; Xiao, K.; Zhang, Z.; Liu, Q.; Hou, G. L.; Li, P.; Tian, Y.; Jiang, L. *Chem. Commun.* **2015**, *51*, 3135.
- (41) Xu, Y. L.; Sui, X.; Guan, S.; Zhai, J.; Gao, L. C. *Adv. Mater.* **2015**, *27*, 1851.
- (42) Vlasiouk, I.; Park, C. D.; Vail, S. A.; Gust, D.; Smirnov, S. *Nano Lett.* **2006**, *6*, 1013.
- (43) Wen, L. P.; Liu, Q.; Ma, J.; Tian, Y.; Li, C. H.; Bo, Z. S.; Jiang, L. *Adv. Mater.* **2012**, *24*, 6193.
- (44) Buchsbaum, S. F.; Nguyen, G.; Howorka, S.; Siwy, Z. S. *J. Am. Chem. Soc.* **2014**, *136*, 9902.
- (45) Wang, G. L.; Bohaty, A. K.; Zharov, I.; White, H. S. *J. Am. Chem. Soc.* **2006**, *128*, 13553.
- (46) An, N.; Fleming, A. M.; White, H. S.; Burrows, C. J. *ACS Nano* **2015**, *9*, 4296.
- (47) Qiu, X. Y.; Yu, H. Z.; Karunakaran, M.; Pradeep, N.; Nunes, S. P.; Peinemann, K. V. *ACS Nano* **2013**, *7*, 768.
- (48) Čeru, S.; Šket, P.; Prislán, I.; Lah, J.; Plavec, J. *Angew. Chem., Int. Ed.* **2014**, *53*, 4881.
- (49) Chailap, B.; Tuntulani, T. *Org. Biomol. Chem.* **2012**, *10*, 3617.
- (50) Lein, G. M.; Cram, D. J. *J. Am. Chem. Soc.* **1985**, *107*, 448.
- (51) van der Wal, P. D.; Sudhölter, E. J. R.; Boukamp, B. A.; Bouwmeester, H. J. M.; Reinhoudt, D. N. *J. Electroanal. Chem. Interfacial Electrochem.* **1991**, *317*, 153.
- (52) Bakker, E.; Simon, W. *Anal. Chem.* **1992**, *64*, 1805.
- (53) Bühlmann, P.; Pretsch, E.; Bakker, E. *Chem. Rev.* **1998**, *98*, 1593.
- (54) Valeur, B.; Leray, I. *Coord. Chem. Rev.* **2000**, *205*, 3.
- (55) Łowicki, D.; Huczyński, A.; Stefańska, J.; Brzezinski, B. *Tetrahedron* **2011**, *67*, 1468.
- (56) Steed, J. W. *Coord. Chem. Rev.* **2001**, *215*, 171.
- (57) Christy, F. A.; Shrivastav, P. S. *Crit. Rev. Anal. Chem.* **2011**, *41*, 236.
- (58) Heins, E. A.; Baker, L. A.; Siwy, Z. S.; Mota, M. O.; Martin, C. R. *J. Phys. Chem. B* **2005**, *109*, 18400.
- (59) Bezrukov, S. M.; Krasilnikov, O. V.; Yuldasheva, L. N.; Berezchkovskii, A. M.; Rodrigues, C. G. *Biophys. J.* **2004**, *87*, 3162.
- (60) Izatt, R. M.; Pawlak, K.; Bradshaw, J. S.; Bruening, R. L. *Chem. Rev.* **1991**, *91*, 1721.
- (61) Pedersen, C. J. *J. Am. Chem. Soc.* **1967**, *89*, 7017.
- (62) Siwy, Z. S. *Adv. Funct. Mater.* **2006**, *16*, 735.
- (63) Wei, C.; Bard, A. J.; Feldberg, S. W. *Anal. Chem.* **1997**, *69*, 4627.
- (64) Siwy, Z. S.; Heins, E.; Harrell, C. C.; Kohli, P.; Martin, C. R. *J. Am. Chem. Soc.* **2004**, *126*, 10850.
- (65) Dang, L. X. *J. Am. Chem. Soc.* **1995**, *117*, 6954.
- (66) Powell, M. R.; Cleary, L.; Davenport, M.; Shea, K. J.; Siwy, Z. S. *Nat. Nanotechnol.* **2011**, *6*, 798.
- (67) Wanunu, M.; Meller, A. *Nano Lett.* **2007**, *7*, 1580.
- (68) Koskela, S. J. M.; Fyles, T. M.; James, T. D. *Chem. Commun.* **2005**, *7*, 945.
- (69) Wang, F.; Han, C. Y.; He, C. L.; Zhou, Q. Z.; Zhang, J. Q.; Wang, C.; Li, N.; Huang, F. H. *J. Am. Chem. Soc.* **2008**, *130*, 11254.
- (70) Yan, X. Z.; Wei, P. F.; Xia, B. Y.; Huang, F. H.; Zhou, Q. Z. *Chem. Commun.* **2012**, *48*, 4968.
- (71) Ashton, P. R.; Ballardini, R.; Balzani, V.; Bělohradský, M.; Gandolfi, M. T.; Philp, D.; Prodi, L.; Raymo, F. M.; Reddington, M. V.; Spencer, N.; Stoddart, J. F.; Venturi, M.; Williams, D. J. *J. Am. Chem. Soc.* **1996**, *118*, 4931.
- (72) Xia, B. Y.; Zheng, B.; Han, C. Y.; Dong, S. Y.; Zhang, M. M.; Hu, B. J.; Yu, Y. H.; Huang, F. H. *Polym. Chem.* **2013**, *4*, 2019.